Mitin, Dmitry; Berdnikov, Yury; Vorobyev, Alexandr; Mozharov, Alexey; Raudik, Sergei; Koval, Olga; Neplokh, Vladimir; Moiseev, Eduard; Ilatovskii, Daniil; Nasibulin, Albert G.; Mukhin, Ivan

Optimization of Optoelectronic Properties of Patterned Single-Walled Carbon Nanotube Films

Published in:
ACS Applied Materials and Interfaces

DOI:
10.1021/acsami.0c14783

Published: 09/12/2020

Document Version
Peer-reviewed accepted author manuscript, also known as Final accepted manuscript or Post-print

Please cite the original version:
Mitin, D., Berdnikov, Y., Vorobyev, A., Mozharov, A., Raudik, S., Koval, O., Neplokh, V., Moiseev, E., Ilatovskii, D., Nasibulin, A. G., & Mukhin, I. (2020). Optimization of Optoelectronic Properties of Patterned Single-Walled Carbon Nanotube Films. *ACS Applied Materials and Interfaces*, *12*(49), 55141-55147. https://doi.org/10.1021/acsami.0c14783

Supporting Information

Optimization of optoelectronic properties of patterned single-walled carbon nanotube films

Dmitry Mitin[*,ǂ,‖,‡], *Yury Berdnikov*[#,‡], *Alexandr Vorobyev*[ǂ], *Alexey Mozharov*[ǂ], *Sergei Raudik*[ǂ,†], *Olga Koval*[ǂ], *Vladimir Neplokh*[ǂ], *Eduard Moiseev*[⊢], *Daniil Ilatovskii*[†], *Albert G. Nasibulin*[**†,§] *and Ivan Mukhin*[ǂ,#]

[ǂ] Saint Petersburg Academic University, 8 Khlopina, bld. 3A, St. Petersburg 194021, Russia

[‖] Peter the Great St. Petersburg Polytechnic University, 29 Politekhnicheskaya, St. Petersburg 195251, Russia

[#] ITMO University, 49 Kronverksky pr., St. Petersburg 197101, Russia

[†] Skolkovo Institute of Science and Technology, Nobel 3, Moscow 121205, Russia

[⊢] National Research University Higher School of Economics, 16 Soyuza Pechatnikov, St Petersburg 190008, Russia

[§] Aalto University, P.O. Box 16100, FI-00076 Aalto, Espoo, Finland.

Corresponding Authors:

*E-mail: mitindm@mail.ru, **E-mail: a.nasibulin@skoltech.ru

S1. Invariance of the transmittance-sheet resistance relation for various grid geometry

In the main body of the paper, we considered the SWCNT grid with the square cell shape to exhibit the relation between initial and final transmittances, T_0 and T, and sheet resistances of patterned and unpatterned SWCNT films, R_s and R_0, respectively. Here we show that eqs. (3) and (4) of the main text are also valid for other grid geometries. In this work we consider the cases only the cases of grids with regular tiling of the plane: with square, triangle and hexagonal cell shape. More complex grid geometries are outside of the scope of the current work.

We also note that by excluding the filling factor f from eqs. (3) and (4) this relation may be formulated as:

$$R_s = \frac{R_0}{1-\sqrt{\frac{T-T_0}{1-T_0}}}. \qquad \text{(S1)}$$

In this section we show that this result is valid not only for the case of square grids, but can be generalized to grids with triangle or hexagonal shape of the elementary cells.

Eq. (3) of the main text is valid in more general case when f is fraction of surface area, covered by the grid. To find the expression for f in the case of triangle and hexagonal grids we consider the cell size p and the size of the area between stripes a, as illustrated in Figure S1. In these terms the area of the entire cell is proportional to p^2 and the area covered by the grid is proportional to $p^2 - a^2$. Triangular and hexagonal cells c are shown in Figure S1 (a and b, respectively), where w is the width of the stripe.

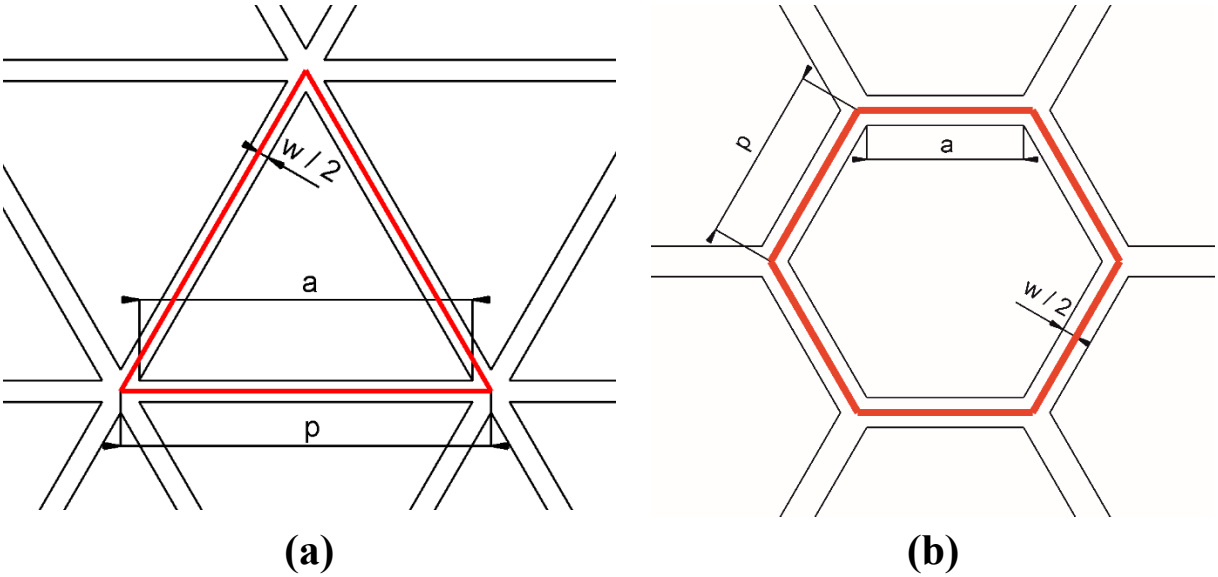

Figure S1. Schematic of the triangle (a) and hexagonal (b) grid cell.

Therefore, similar to the case of rectangular grid, f can be found as

$$f = \frac{p^2-a^2}{p^2} = 1 - \left(\frac{a}{p}\right)^2 \qquad \text{(S2)}$$

Equation S2 is valid in both the cases of triangle and hexagonal grids.

Next we consider eq. (4) of the main text in hexagonal and triangle grid geometries. To simplify the calculation of the sheet resistance we have introduced rectangular areas, including cells of triangular and hexagonal shapes (dashed lines on Figure S2 a and b, respectively). Sheet resistance of a grid cell R_s^i can be find as cell resistance R_{cell}^i multiplied by cell width and divided by length, where index $i = tri$ or hex for triangle or hexagonal grid, respectively:

$$R_s^{tri} = R_{cell}^{tri} \frac{p/2}{\sqrt{3}p/2} \quad \text{(S3)}$$

for triangle grid and

$$R_s^{hex} = R_{cell}^{hex} \frac{3p/2}{\sqrt{3}p} \quad \text{(S4)}$$

for hexagonal grid.

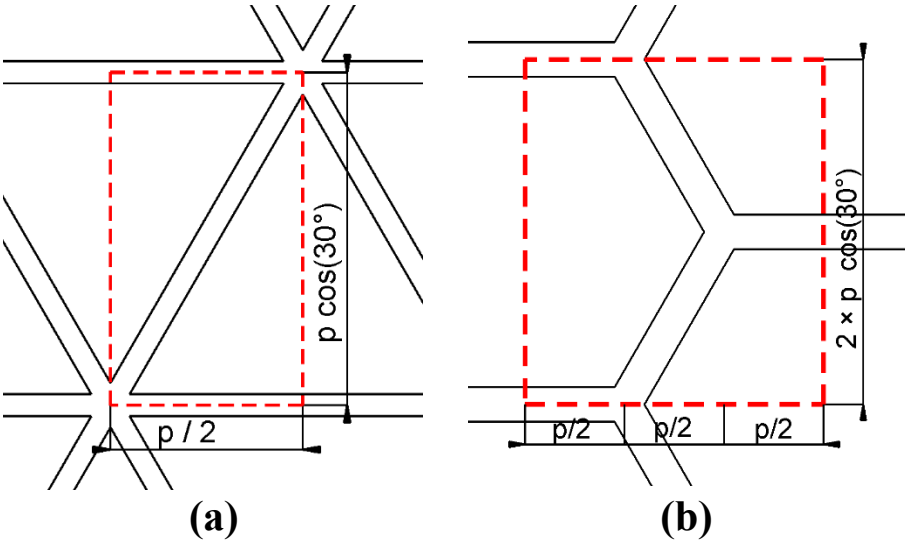

Figure S2. Schematic of rectangular areas for sheet resistance calculation for triangle (a) and hexagonal (b) grid cell.

The cell resistances are defined by linewidth w:

$$R_{cell}^{tri} = R_0 \frac{p}{w} \quad \text{(S5)}$$

and

$$R_{cell}^{hex} = R_0 \frac{p}{w/2}. \quad \text{(S6)}$$

Thus we obtain:

$$R_s^{tri} = R_0 \frac{p}{\sqrt{3}w} \quad \text{(S7)}$$

$$R_s^{hex} = R_0 \frac{\sqrt{3}p}{w}. \quad \text{(S8)}$$

The linewidth w is related to a and p differently in hexagonal and triangle grids:

$$w = \frac{p-a}{\sqrt{3}} \quad \text{(S9)}$$

in triangle grid and

$$w = \sqrt{3}(p-a) \quad \text{(S10)}$$

in hexagonal grid.

Thus both eq. S3 and S4 yield $R_S^i = R_0 \frac{p}{p-a}$, which in view of eq. S2 means:

$$R_S^i = R_0 \frac{1}{1-\sqrt{1-f}} \quad \text{(S11)}$$

Thus we have shown that eq. (3) and eq. (4) are valid in the cases of hexagonal and triangle grids.

S2. T(f) dependence

Figure 2 shows the dependence of the sheet resistance of patterned and continuous SWCNT films on the transmittance of SWCNT layers before the patterning. However, in our approach we obtain the grids with the target transmittance by varying the linewidth to period ratio, or in other terms, the filling factor f. Therefore it is also could be useful from practical point of view to consider the dependence of grid transmittance as the function of f. Figure S3a shows the $T(f)$ dependences given by eq. (6) of the main text for the sheet resistances of patterned films of $R_s = 10$ and $30\ \Omega/\square$ (solid lines) and the same $\alpha\rho$ as Figure 1e. Dashed horizontal lines mark the transmittances of the continuous films corresponding to $f = 1$. Dotted line shows the solution of eq. (7) of the main text expressed in terms of T and f using eqns. (3) and (4). One can see that the part of the $T(f)$ curve to the left from the intersection with the dotted line shows T higher than the transmittance of continuous film for a given sheet resistance.

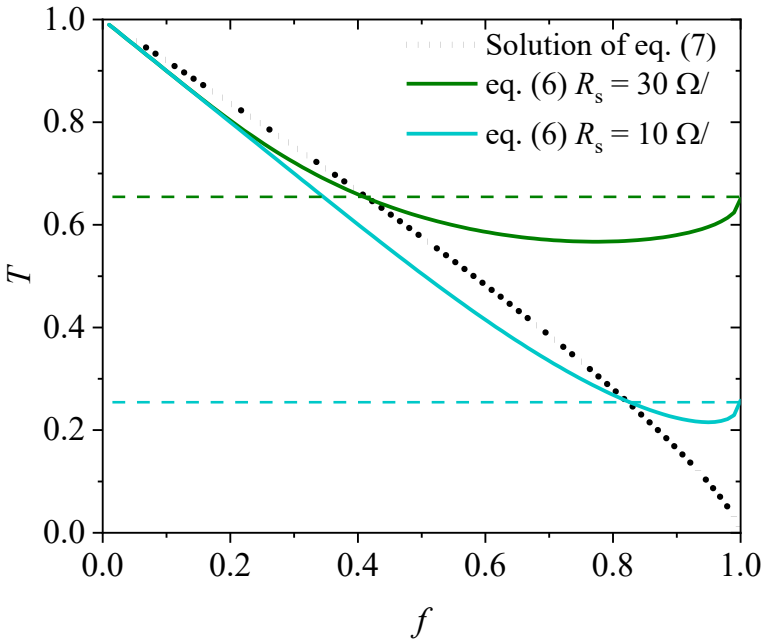

Figure S3. Transmittance of patterned SWCNT films with sheet resistance of $R_s = 10$ and $30\ \Omega/\square$.

S3. Analytical solution of eq. (7) in linear approximation

We can rewrite eq. (7) of the main text to express the correlation between T_0 and T using eq. (8):

$$\frac{ln\,T}{ln\,T_0} = 1 - \sqrt{1 - \frac{1-T}{1-T_0}}. \qquad \text{(S12)}$$

In the limit of highly transparent grid ($T \to 1$) series expansions with a small $1 - T$ gives

$$ln\,T = ln\big(1 - (1-T)\big) \approx -(1-T) - \frac{1}{2}\cdot(1-T)^2 + \cdots \qquad \text{(S13a)}$$

$$\sqrt{1 - \frac{1-T}{1-T_0}} \approx 1 - \frac{1}{2}\cdot\frac{1-T}{1-T_0} - \frac{1}{8}\cdot\left(\frac{1-T}{1-T_0}\right)^2 + \cdots \qquad \text{(S13b)}$$

With the limitation by the first-order terms, eq. (S12) can be rewritten as

$$-\frac{1-T}{ln\,T_0} = 1 - 1 + \frac{1}{2}\cdot\frac{1-T}{1-T_0}. \quad \text{(S14)}$$

The both sides of eq. (S14) can be divided by $1-T$ to eliminate the dependence on T when $T \to 1$ but stays less than unity. This approximation corresponds to T_0 value fixed to T_0^*:

$$\frac{ln\,T_0^*}{1-T_0^*} = -2 \;=>\; T_0^* = T_0|_{T\to 1} = -\frac{1}{2}W(-2\cdot e^{-2}) \approx 0.2032, \quad \text{(S15)}$$

where $W(z)$ is the Lambert function.

By limiting to the second-order terms, eq. (S12) can be rewritten as

$$-\frac{1-T}{ln\,T_0}\left(1+\frac{1}{2}\cdot(1-T)\right) = 1 - 1 + \frac{1}{2}\cdot\frac{1-T}{1-T_0}\cdot\left(1+\frac{1}{4}\cdot\frac{1-T}{1-T_0}\right), \quad \text{(S16)}$$

which after the simplification leads to

$$-(3-T) = \frac{ln\,T_0}{1-T_0} + \frac{1}{4}\cdot\frac{ln\,T_0}{1-T_0}\cdot\frac{1-T}{1-T_0}. \quad \text{(S17)}$$

Linearization of the terms depending on T_0 gives:

$$\frac{ln\,T_0}{1-T_0} = \frac{ln\left(T_0^*-(T_0^*-T_0)\right)}{1-T_0} = \frac{ln\,T_0^*}{1-T_0} + \frac{ln\left(1-\left(1-{}^{T_0}/_{T_0^*}\right)\right)}{1-T_0},$$

$$\frac{ln\,T_0^*}{1-T_0} = \frac{ln\,T_0^*}{1-T_0^*}\cdot\frac{1}{1+\frac{T_0^*-T_0}{1-T_0^*}} = \frac{-2}{1+\frac{T_0^*-T_0}{1-T_0^*}} \approx -2 + 2\cdot\frac{T_0^*-T_0}{1-T_0^*}, \quad \text{(S18)}$$

$$\frac{ln\left(1-\left(1-{}^{T_0}/_{T_0^*}\right)\right)}{1-T_0} \approx -\frac{1}{T_0^*}\cdot\frac{T_0^*-T_0}{1-T_0^*}$$

$$=>\; \frac{ln\,T_0}{1-T_0} \approx -2 + 2\cdot\frac{T_0^*-T_0}{1-T_0^*} - \frac{1}{T_0^*}\cdot\frac{T_0^*-T_0}{1-T_0^*} = -2 - \frac{1-2T_0^*}{T_0^*}\cdot\frac{T_0^*-T_0}{1-T_0^*}.$$

Keeping only linear to 1-T and T_0^*-T_0 terms one can obtain:

$$-(3-T) = \frac{ln\,T_0}{1-T_0} + \frac{1}{4}\cdot\frac{ln\,T_0}{1-T_0}\cdot\frac{1-T}{1-T_0} \approx -2 - \frac{1-2T_0^*}{T_0^*}\cdot\frac{T_0^*-T_0}{1-T_0^*} - \frac{1}{2}\cdot\frac{1-T}{1-T_0^*}. \quad \text{(S19)}$$

Regrouping the terms, we recover the correlation between $T$and T_0 in the linear approximation at $T \to 1$:

$$1 - T = \frac{2}{T_0^*}\cdot(T_0^* - T_0). \quad \text{(S20)}$$

Taking into account the correlation between the transmittance and the equivalent sheet resistance, eq. (S20) can be expressed in the form of R=f(T_0):

$$R_{eq} = \frac{-\alpha\rho}{ln\,T} = \frac{-\alpha\rho}{ln\left(1-{}^{2}/_{T_0^*}\cdot(T_0^*-T_0)\right)}. \quad \text{(S21)}$$

S4. I-V characteristics of SWCNT stripes

The I-V characteristics of continuous and patterned SWCNT films and stripes were measured using probe station and Keithley 2400 source meter in -1…+1 V range. To calculate the

surface resistance of the continuous and patterned SWCNT films the 2-probe method was used. Typical I-V curves of SWNCT stripes with different widths (w) and lengths (l) are presented on figure S4.

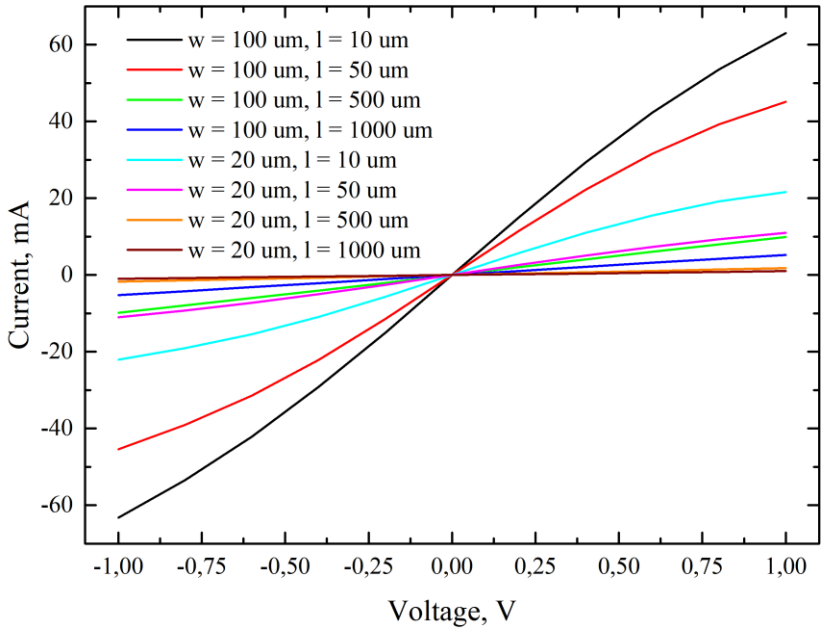

Figure S4. I-V curves of SWNCT stripes (90 nm thickness) with different widths (w) and lengths (l)

S5. Bending test

Since flexibility is one of the most important advantages of SWCNT films, the patterned layers were encapsulated in 1 mm thick polydimethylsiloxane PDMS to study the impact of bending on the grid conductivity. During the flexibility tests, the samples were bent around quartz tubes with the diameters (D) from 67.5 down to 22.0 mm. Figure S5 (a) and (b) show the sample view sketch and the resistance variation ($\Delta R/R$) in the bend-release tests, correspondingly. The strain in Figure S5 (b) was evaluated as PDMS film thickness divided by the quartz tube diameter. We observed a very moderate increase of resistance below 5% under the strain up to 4 %, which is comparable with the previous results for continuous SWCNT films [1] and shows the improvement in comparison with the previous reports on patterned SWCNT films [2].

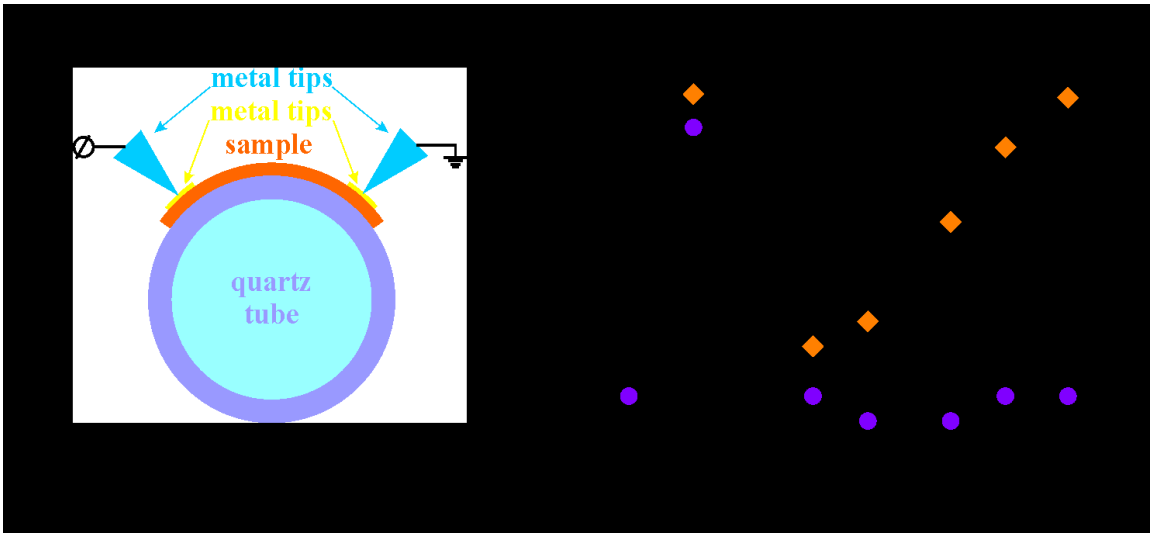

Figure S5. (a) Sample view sketch and (b) variation of resistance in bend-release tests.

References

(1) Trottier, C. M.; Glatkowski, P.; Wallis, P.; Luo, J. Properties and Characterization of Carbon-Nanotube-Based Transparent Conductive Coating. *J. Soc. Inf. Disp.* **2005**, *13* (9), 759. https://doi.org/10.1889/1.2080514.

(2) Fukaya, N.; Kim, D. Y.; Kishimoto, S.; Noda, S.; Ohno, Y.; Engineering, Q.; Chemistry, A. One-Step Sub-10 μ m Patterning of Carbon-Nanotube Thin Films For. *ACS Nano* **2014**, *8* (4), 3285–3293.